Available online at www.sciencedirect.com

ScienceDirect

Journal of the European Ceramic Society 28 (2008) 1917–1922

www.elsevier.com/locate/jeurceramsoc

Reaction synthesis and characterisation of lanthanum silicon nitride

Z. Lenčéš [a,*], L. Benco [a,b], J. Madejová [a], Y. Zhou [c], L. Kipsová [a], K. Hirao [c]

[a] *Institute of Inorganic Chemistry, Slovak Academy of Sciences, Dúbravská cesta 9, 845 36 Bratislava, Slovakia*
[b] *Fakultät für Physik and Center for Computational Materials Science, Universität Wien, Sensengasse 8, A-1090 Wien, Austria*
[c] *National Institute of Advanced Industrial Science and Technology (AIST), 2266-98 Shimo-Shidami, Moriyama-ku, Nagoya 463-8560, Japan*

Received 23 August 2007; received in revised form 19 November 2007; accepted 25 November 2007
Available online 7 February 2008

Abstract

The synthesis of lanthanum silicon nitride ($LaSi_3N_5$) by direct nitridation of LaSi/Si/Si_3N_4 powder mixture at 1400 °C is described. Stepwise heat treatment schedule was adopted for the synthesis of $LaSi_3N_5$ powder, on the basis of TG–DTA measurements. Except temperature and nitrogen pressure also the ratio of constituents LaSi/Si/Si_3N_4 has an influence on the exothermicity of the reaction and consequently on the final phase composition of the product. Silicon particle size $d \leq 1$ μm is preferable to decrease the time of nitridation. On the other hand, the reaction system must be diluted with Si_3N_4 to avoid the overheating of powder mix and melting of silicon. When starting from binary LaSi/Si_3N_4 powder mixture, additional nitridation at higher temperature (1550 °C) was necessary to obtain single phase $LaSi_3N_5$ powder. The oxygen content of as-synthesized powders was in the range 1.0–1.2 wt%.

The lattice parameters and diffraction pattern of $LaSi_3N_5$ have been calculated and compared with experimental data. The infrared spectra of $LaSi_3N_5$ have been measured and partly described.

Keywords: $LaSi_3N_5$; Reaction synthesis; Spectroscopy; Nitridation' powders – solid state reaction

1. Introduction

Ternary nitrides have recently been widely studied, because they may display a wider variety of useful properties compared to the binary nitrides. Silicon-based ternary nitrides like $MgSiN_2$ and $LaSi_3N_5$ are intensively studied as an alternative material for the substrates of the integrated circuits,[1–5] as host lattices for light emitting phosphors,[6–12] semiconductors, etc. The functional properties with a combination of good strength, fracture toughness and hardness make both ternary nitrides suitable for several industrial applications. Contrary to binary nitrides (Mg_3N_2 and LaN) the ternary nitrides are stable in air for long periods of time. $LaSi_3N_5$ is resistant to aqua regia ($HNO_3 + 3HCl$),[13] and can be used at higher temperatures in fluorine containing environment compared to nickel alloys.[14]

Several synthesis procedures have been utilized to make $LaSi_3N_5$ powder. The compound has been prepared by a reaction between Si_3N_4 and La_2O_3 at 2000 °C under 5 MPa nitrogen pressure[15]; by hot pressing of Si_3N_4 and LaN at 1830 °C for 1 h, under 28 MPa load[14]; by direct reaction of Si_3N_4 and LaN at 1700 °C for 30 min, under 14.7 MPa nitrogen pressure[16]; by direct reaction of $LaSi_3$ alloys with nitrogen at 1500 °C and 0.1 MPa N_2 pressure for one week[13]; by carbothermal reduction and nitridation (CRN) of La_2O_3 and SiO_2 with carbon,[17] or by CRN of lanthanum acetate and tetraethoxysilane with carbon.[17,18] The oxygen content varied depending on the method of preparation between 1 and 2.5 wt%.

The purpose of this work is to produce $LaSi_3N_5$ powder from a mixture of LaSi, Si and Si_3N_4 starting materials with an intention to shorten the time of nitridation and make the process cost-effective.

2. Experimental

Commercial powders of LaSi (Kojundo Chemical Laboratory Co., Japan), Si (99%, grain size <1 μm, Kojundo Chem. Lab. Co., Japan), and α-Si_3N_4 (grade SN-E10, Ube Industries Ltd., Japan) were used for the synthesis of $LaSi_3N_5$ powder. The starting powder compositions were calculated according to the

---

[*] Corresponding author. Tel.: +421 2 59410408; fax: +421 2 59410444.
E-mail address: uachlenc@savba.sk (Z. Lenčéš).

0955-2219/$ – see front matter © 2008 Elsevier Ltd. All rights reserved.
doi:10.1016/j.jeurceramsoc.2007.11.017

following general reaction:

$$\mathrm{LaSi} + (2\text{–}3x)\mathrm{Si} + x\mathrm{Si_3N_4} + (5/2\text{–}2x)\mathrm{N_2} = \mathrm{LaSi_3N_5} \qquad (1)$$

Two different compositions have been studied in details: binary system LaSi/Si_3N_4 (sample LSN-2, with $x = 2/3$) and ternary LaSi/Si/Si_3N_4 starting mixture (sample LSN-3, $x = 0.55$). Owing to the partial evaporation of metals during nitridation, 5 wt% excess of LaSi was added to both mixtures.[19]

The powders were mixed in Si_3N_4 planetary ball mill in toluene for 2 h. The dried and sieved powders were placed into a BN crucible and heat-treated in an alumina-tube furnace (Koyo Thermo Systems Co., Tenri-shi, Japan) to 1400 °C with 1.5 L/min, high-purity nitrogen-gas flow.

Differential thermal analysis (DTA) and thermogravimetry (TG) were conducted up to 1400 °C (model Thermo-Plus TG 8120, Rigaku Co., Tokyo, Japan) using alumina sample holders and applying a constant heating rate of 5 °C/min, in a flowing nitrogen-gas atmosphere. The phase composition of the nitrided materials was investigated by powder X-ray diffraction (Bragg-Brentano geometry and Cu Kα radiation, model RINT2500, Rigaku Co., Japan). Precise XRD measurements were conducted also in Debye–Scherrer transmission geometry and using Co Kα radiation (STOE Stadi-P, Germany). The samples were rotated during measurements and the data were collected on a position-sensitive detector. The oxygen and nitrogen contents of synthesized $LaSi_3N_5$ powders were also determined (model TC-436, LECO Co., USA).

The KBr pressed disc technique (1 mg of sample and 200 mg of KBr) was used for infrared spectroscopy. The spectra were obtained on a Nicolet Magna 750 FTIR spectrometer, equipped with an IR source and KBr beam splitter. The scans were recorded with a resolution of 4 cm^{-1}.

Structure optimizations were performed using the *ab initio* total-energy program VASP[20,21] based on density functional theory (DFT). Full relaxation of all the atomic positions is performed via a conjugate-gradient algorithm.

3. Results and discussion

3.1. Thermal analysis

The TG–DTA curves of samples LSN-2 and LSN-3 are shown in Fig. 1. The exothermic reaction starts at 695 °C in sample LSN-2 and at 710–715 °C in samples with composition LSN-3. The reaction attenuates at 863 °C in both powders and accelerates again at 1185–1195 °C. The two observed exothermic reactions are most probably related to the eutectics in the La–Si binary system: $T_E(\mathrm{La\text{–}La_5Si_3}) = 722 \pm 9\,°\mathrm{C}$ and $T_E(\mathrm{LaSi_{2-x}\text{–}Si}) = 1205 \pm 7\,°\mathrm{C}$.[22] It is well known that the formation of liquid phase promotes the nitridation of silicon.[23,24] On the other hand, it is necessary to avoid the local overheating of the reaction system due to the exothermic nitridation reaction. From this reason the starting mixture contained 41 vol% (LSN-3) or 49 vol% (LSN-2) of Si_3N_4 as diluting agent and was beneficial for the production of fine homogeneous $LaSi_3N_5$ powder. The DTA curve of sample LSN-3 shows additional inflex point at 1335–1340 °C, followed by exothermic effect at 1360–1365 °C. The heat was generated continuously in sample LSN-2 from 1195 °C up to the final 1400 °C.

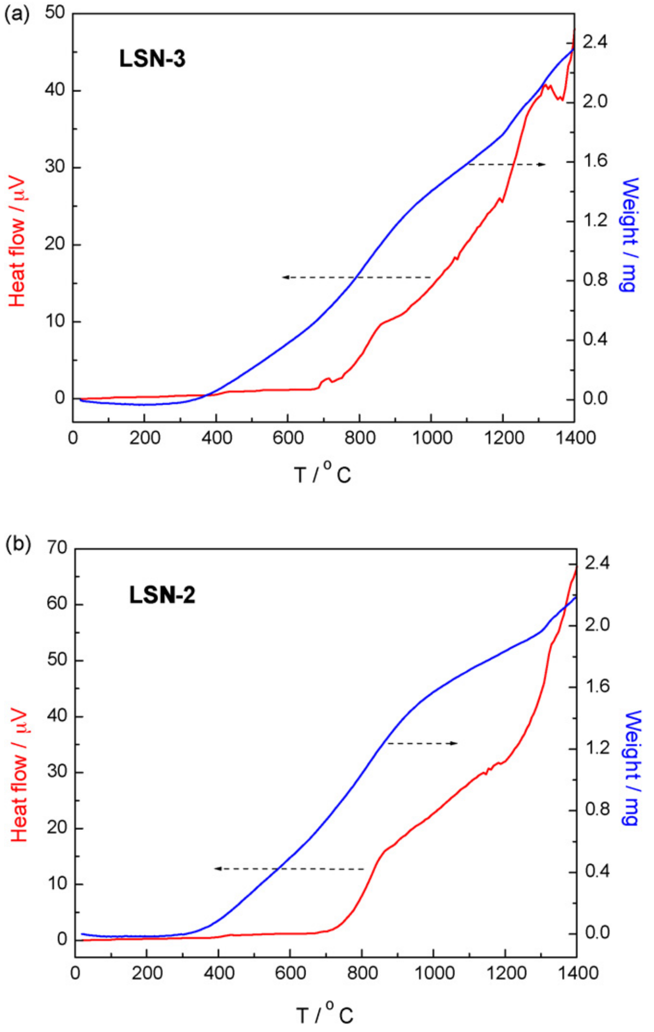

Fig. 1. TG–DTA curves of samples (a) LSN-3 and (b) LSN-2.

The TG curves of all samples showed that the weight gain starts at ∼350 °C and gradually increases until the maximum temperature 1400 °C (Fig. 1). The weight gain up to ∼1200 °C is due to the formation of LaN, which is confirmed by XRD analysis of samples nitrided up to 800, 900 and 1220 °C for 1 h. The phase analysis of all samples suggests the following intermediate products formation:

$$3\mathrm{LaSi} + \mathrm{N_2} \rightarrow 2\mathrm{LaN} + \mathrm{LaSi_2} + \mathrm{Si} \qquad (2a)$$

$$2\mathrm{LaSi_2} + \mathrm{N_2} \rightarrow 2\mathrm{LaN} + 4\mathrm{Si} \qquad (2b)$$

$$3\mathrm{Si} + 2\mathrm{N_2} \rightarrow \mathrm{Si_3N_4} \qquad (3)$$

and the final reaction:

$$\mathrm{LaN} + \mathrm{Si_3N_4} \rightarrow \mathrm{LaSi_3N_5} \qquad (4)$$

Reaction (2a) was confirmed by the analysis of sample LSN-2, which contained also Si and $LaSi_{2-x}$ in the product nitrided at 900 °C, although the only starting powders were LaSi and Si_3N_4.

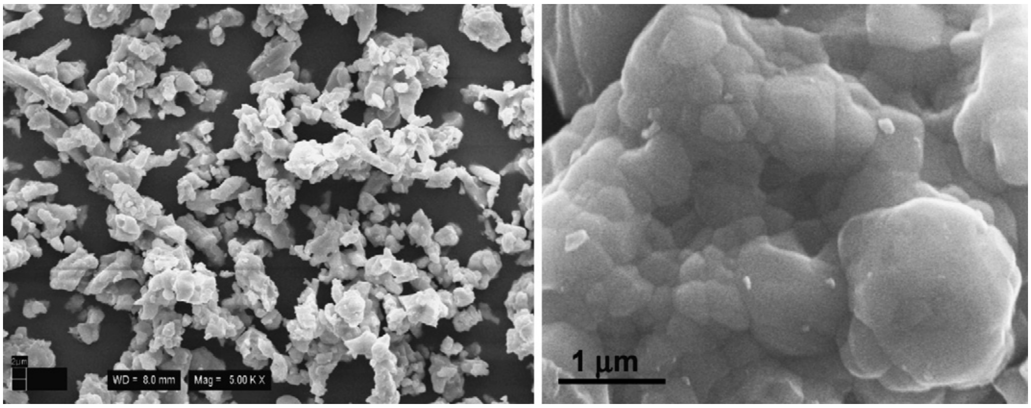

Fig. 2. SEM micrographs of sample LSN-3.

The advantage of in situ-formed Si is the finer particle size and faster nitridation compared to the raw Si powder ($d_{50} \leq 1$ µm, but some particles were in the range of 10 µm). The nitridation of silicon (both intentionally added and in situ formed) according to reaction (3) is responsible for further increase of weight up to the final temperature of 1400 °C. The simultaneous formation of $LaSi_3N_5$ at temperatures $T > 1350$ °C by reaction (4) does not contribute to the weight gain. However, the formation of $La_3Si_6N_{11}$ cannot be excluded, which might cause certain differences between the calculated and real weight gain (and nitrogen content) of the nitrided product.

3.2. Powder characteristics and elemental analysis

The synthesized $LaSi_3N_5$ powder had a light-grey colour. The morphology of unmilled powder is shown in Fig. 2. The size of agglomerates is 2–10 µm, while the individual particle size is 0.2–1 µm. The crystallite size determined from the half width of XRD peak intensities according to the Scherrer equation is in the range 110–140 nm.

The oxygen and nitrogen content of the analyzed samples are listed in Table 1. The nitrogen content of all samples is close to the theoretical 23.88 wt%. Slightly lower values are due to the presence of oxygen and small amount of $La_3Si_6N_{11}$ and LaSi phases. The latter might cause the greyish colour. The nitrogen content in $La_3Si_6N_{11}$ is lower compared to $LaSi_3N_5$, only 20.84 wt%.

The oxygen content in both LSN samples is in correlation with the oxygen impurity in the starting powders: 1.32 wt% in α-Si_3N_4, 1.28 wt% in Si and 0.74 wt% in LaSi, and with the fact that the nitridation was conducted in alumina tube furnace.

Table 1
Experimental and theoretical content of nitrogen and oxygen in the synthesized $LaSi_3N_5$ powders

Powder	N (wt%)	O (wt%)
LSN-2	23.08	1.01
LSN-3	23.27	1.06
$LaSi_3N_5$ (Inoue et al.[15])	20.93	0.67
$LaSi_3N_5$ (theoretical)	23.88	–

3.3. Phase composition

The XRD patterns of powder products are shown in Fig. 3. Samples LSN-2a and LSN-3 were heated to 1400 °C. While $LaSi_3N_5$ was the major phase in sample LSN-3, the intermediate products LaN and Si_3N_4 had the strongest diffraction intensity in LSN-2a sample. $LaSi_3N_5$ was the minor phase. By further annealing of this sample at 1550 °C for 1 h, under 0.8 MPa N_2 atmosphere $LaSi_3N_5$ powder was prepared (sample LSN-2b).

The XRD patterns of LSN-2b and LSN-3 samples are similar and the major phase is $LaSi_3N_5$. However, there were still some unidentified weak diffractions peaks. From this reason the XRD pattern of the DFT-relaxed structure of $LaSi_3N_5$ has been calculated and compared with our experimental data and with Powder Diffraction File No. 42-1144. The results are shown in Fig. 4. Except of weak peaks at $2\Theta = 30.9°$ and 39.8°, which can belong to LaSi (PDF 89-1714) and Si (PDF 35-1158), the other diffractions are from the $LaSi_3N_5$ crystal planes.

The XRD results showed that from ternary LaSi/Si/Si_3N_4 system nearly single phase $LaSi_3N_5$ can be prepared by nitridation at 1400 °C, while the binary LaSi/Si_3N_4 system should be annealed at higher temperature. Due to the exothermic character of nitridation reaction, the reason is most probably the difference

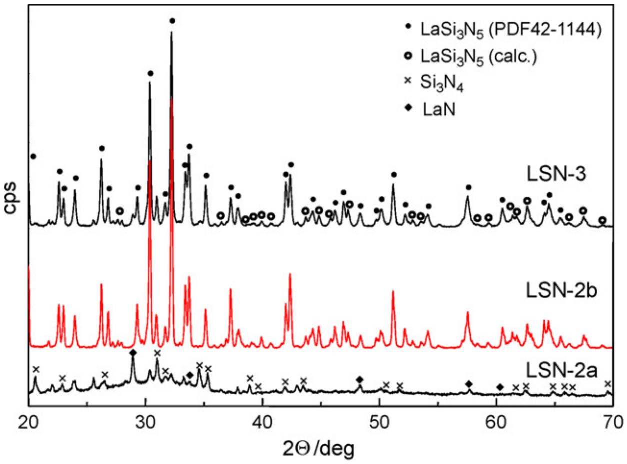

Fig. 3. XRD patterns of samples after nitridation at 1400 °C (LSN-2a and LSN-3) and at 1550 °C (LSN-2b).

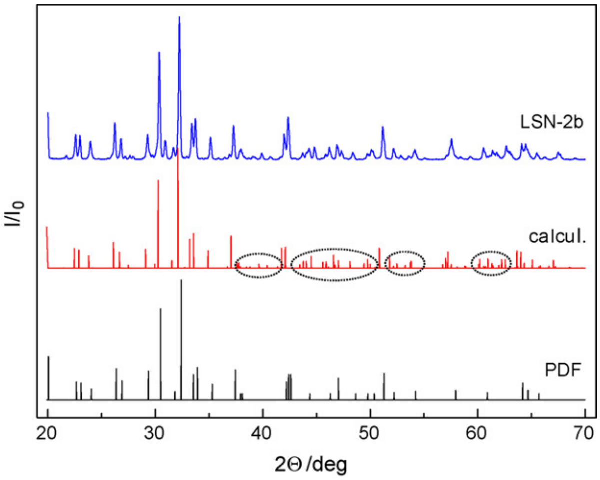

Fig. 4. Comparison of the experimental XRD pattern of $LaSi_3N_5$ (sample LSN-2b) with the calculated XRD profile and PDF 42-1144 of $LaSi_3N_5$.

in the generated heat by reaction

$$\mathrm{LaSi} + (2\text{–}3x)\mathrm{Si} + x\mathrm{Si_3N_4} + (5/2\text{–}2x)\mathrm{N_2} = \mathrm{LaN} + \mathrm{Si_3N_4} \tag{5}$$

for $x = 0.55$ (ternary system) and $x = 2/3$ (binary system). The enthalpies of reaction for both x values are shown in Fig. 5. The standard enthalpy of formation $\Delta H^{\circ}_{\mathrm{f}}$ (LaSi) = $-73.9\,\mathrm{kJ\,mol^{-1}}$ was taken from Meschel et al.,[25] and the temperature function $H^{\circ}(T) - H^{\circ}$ (298 K) from Bolgar et al.[26] The other thermodynamic data are from JANAF Thermochemical Tables[27] and MALT2 database. The results show that the exothermic character of reaction for ternary system is higher (more negative). The evolved heat can support the formation of $LaSi_3N_5$ according to reaction (4), while for binary system additional external heat is necessary to complete the reaction.

3.4. Infrared spectroscopy

Owing to the presence of amorphous hump in the XRD pattern of sample LSN-2a, the nitrided products have been analyzed also by infrared (FTIR) spectroscopy. The room temperature FTIR absorption spectra are shown in Fig. 6. The IR spectrum of LSN-2a sample resembles that of α-Si_3N_4 (commercial Ube SN-E10; measured in lab), which is also shown for the comparison in Fig. 6a. The majority of the bands belong to Si–N stretching and bending/rocking vibrations and their positions are in agreement with the published data for α-Si_3N_4 (Table 2).[28–31] In addition to Si_3N_4 bands a broad absorption near $720\,\mathrm{cm^{-1}}$ appears in the spectrum of the sample LSN-2a. This band may indicate the creation of the La–N bonds.

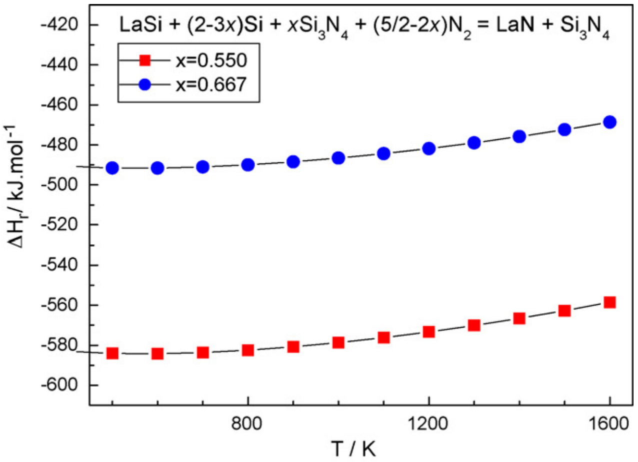

Fig. 5. Enthalpies of reactions for x values 0.55 and 0.667 in reaction (5). The ternary LaSi/Si/Si_3N_4 system yields more exothermic reaction.

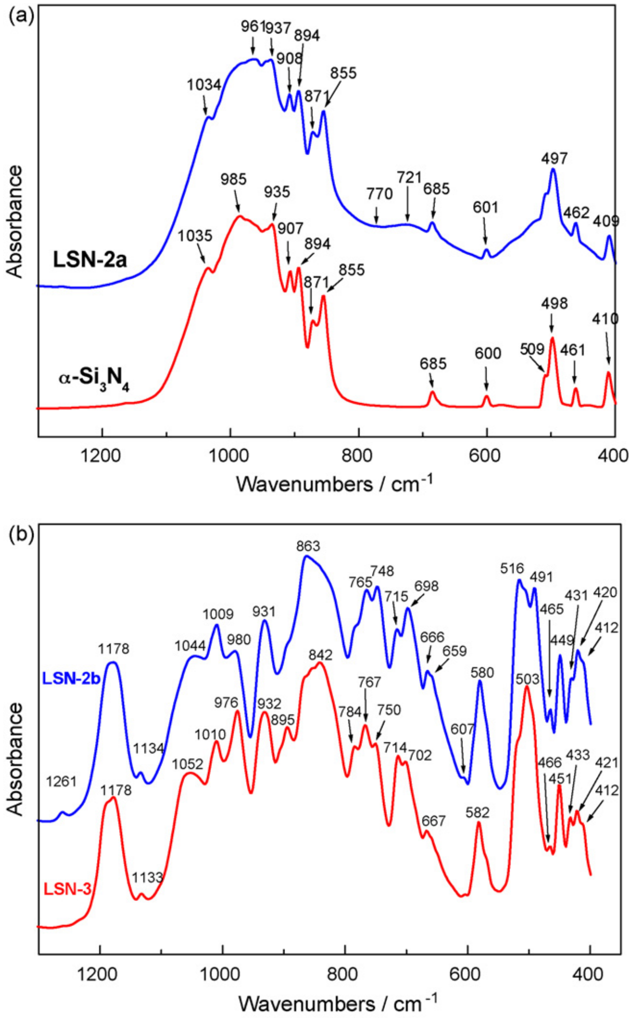

Fig. 6. Infrared spectra of (a) sample LSN-2a and commercial Ube SN-E10 α-Si_3N_4 powder, (b) samples LSN-2b and LSN-3 (both have $LaSi_3N_5$ crystalline phase composition).

The FTIR spectra of $LaSi_3N_5$ powders (samples LSN-2b and LSN-3 in Fig. 6b) are different from that of LSN-2a sample. While a broad band near $960\,\mathrm{cm^{-1}}$ and several peaks in the 900–850 $\mathrm{cm^{-1}}$ region dominates in the spectrum of LSN-2a, the shape of the $LaSi_3N_5$ spectrum is more complicated. Lot of well-resolved bands indicates pronounced variability in the bonding configuration in $LaSi_3N_5$, clearly different from that of LSN-2a. Majority of the bands in the $LaSi_3N_5$ spectrum, i.e. bands in the 1000–800 $\mathrm{cm^{-1}}$ region and below $500\,\mathrm{cm^{-1}}$ belong to Si–N vibrations (Table 2). However, different inten-

Table 2
Position of bands in IR-spectra of LSN samples together with published data for α-Si_3N_4

LSN-2a ν (cm^{-1})	LSN-2b ν (cm^{-1})	LSN-3 ν (cm^{-1})	α-Si_3N_4[a] ν (cm^{-1})	α-Si_3N_4[b] ν (cm^{-1})	α-Si_3N_4[c] ν (cm^{-1})	α-Si_3N_4[d] ν (cm^{-1})	α-Si_3N_4[e] ν (cm^{-1})	Assign.[32,33]
	1178	1178						
	1134	1133						
1035	1044	1052	1035	1040	1040	1030	1050	SiN_4
	1009	1010		995				
963	980	976	985				970–980	SiN_4
938	931	932	936	935	950	940		
908			908	909	906	900	900–910	SiN
894		895	894	895	893	880		SiNSi
873	863	842	869	874	872			SiN
855			855	855	855	850	850	SiNSi
	782	784						
	765	767						
	748	750						
727[f]	715	714				720		
686	698	702	684	688	685	680		
	666	667				665		
601			600	600	605	600		
575[f]	580	582	578	580	584	572	580–585	SiN
509	516			512	509	510		
497		503	497	499	496		500–505	SiN
	491				485	490		SiN
461	465	466	461	463	461	460	470	SiN
	449	451	442	440	445		445	SiN
	431	433				432		
	420	421					420	SiN
410	412	412	409	412	410			

[a] Grade Ube SN-E10.
[b] Wada et al.[28].
[c] Kislyj et al.[29].
[d] Nyquist et al.[30].
[e] Andrievskij et al.[31].
[f] Broad band.

sities and positions of the bands when compared to α-Si_3N_4 suggest diverse environment of the Si–N bonds. Moreover, a strong absorption band at 1178 cm^{-1} together with intensive absorption in the 800–500 cm^{-1} region is seen only in the spectrum of $LaSi_3N_5$. The assignment of the individual bands is not clear yet, but it is supposed that these new bands are connected with both, vibrations of Si–N bonds in structural arrangement characteristic for $LaSi_3N_5$, and with vibrations of the bonds in which La atoms are involved, e.g. La–N. Inoue[16] has already reported that there are two types of nitrogen environments in $LaSi_3N_5$: (i) the first type nitrogen is surrounded by three silicons in a coordination similar to α-Si_3N_4, (ii) the second type nitrogen is surrounded by two silicon and two lanthanum atoms.

3.5. *Lattice parameters*

To calculate the lattice parameters of crystalline $LaSi_3N_5$ precise XRD measurements of sample LSN-3 were carried out on STOE Stadi-P equipment with position-sensitive detector (Debye–Scherrer transmission geometry, Co Kα radiation). The measurement conditions were: step 0.010°; rate 0.15°/min, in the range $2\Theta = 20°–70°$. The results are summarized in Table 3 together with the published lattice parameters,[13,15,18] and values calculated in this work from the optimized structure of $LaSi_3N_5$.

The experimental lattice parameters (sample LSN-3) are close to the values reported by Woike and Jeitschko.[13] Slightly higher values of calculated lattice parameters are a consequence of the use of the GGA approach to the functional for the exchange and correlation of electrons. While local density approximation (LDA) leads to too short lattice parameters, the semi-local GGA leads to slightly longer lattice vectors, usually closer to experimental values. The differences in experimental results can be caused by the residual oxygen in the evaluated samples

Table 3
Experimental and calculated lattice parameters of $LaSi_3N_5$ (space group $P2_12_12_1$).

Source	*a* (nm)	*b* (nm)	*c* (nm)
Inoue et al.[15]	0.7838	1.1236	0.4807
Woike and Jeitschko[13]	0.7853	1.1264	0.4817
Hatfield et al.[18]	0.7855	1.1267	0.4818
LSN-3	0.78489	1.12680	0.48144
Calculated	0.79030	1.13382	0.48507

(Table 1). It has already been shown in our previous papers[34,35] that the O/N substitution cause a local expansion of the structure.

4. Conclusions

Almost single phase $LaSi_3N_5$ powder was obtained by direct nitridation of $Si/LaSi/Si_3N_4$ powder mixture. Stepwise heat treatment schedule up to 1400 °C in flowing nitrogen atmosphere was adopted for the synthesis of $LaSi_3N_5$ powder, on the basis of TG–DTA measurements. The ratio of constituents $Si/LaSi/Si_3N_4$ had an influence on the exothermicity of the reaction and consequently on the final phase composition of the products. When starting from binary $LaSi/Si_3N_4$ powder mixture, additional nitridation at higher temperature (1550 °C) was necessary to obtain single phase $LaSi_3N_5$ powder.

Additionally, the lattice parameters and diffraction patterns have been calculated and the infrared spectra of $LaSi_3N_5$ have been measured and partly described.

Although the oxygen content of as-synthesized powders was in the range 1.0–1.2 wt%, the synthesis method allows to obtain lower oxygen level. The in situ preparation of LaN and the part of Si_3N_4 is advantageous, because the in situ-formed binary nitrides are not exposed to oxygen or humidity before the final reaction yielding ternary $LaSi_3N_5$.

Acknowledgements

This work was supported by JSPS Japan, by the National Slovak Grant Agency VEGA, project No. 2/7171/27 and APVV-0448-06. The financial support of the Austrian Science Fund under project No. P17020-PHYS is also acknowledged.

References

1. Groen, W. A., Kraan, M. J. and de With, G., Preparation, microstructure and properties of $MgSiN_2$ ceramics. *J. Eur. Ceram. Soc.*, 1993, **12**, 413–420.
2. Hintzen, H. T., Swaanen, P., Metselaar, R., Groen, W. A. and Kraan, M. J., Hot-pressing of $MgSiN_2$ ceramics. *J. Mater. Sci. Lett.*, 1994, **13**, 1314–1316.
3. Davies, I. J., Uchida, H., Aizawa, M. and Itatani, K., Physical and mechanical properties of hot-pressed magnesium silicon nitride compacts with yttrium oxide addition. *Inorg. Mater. Jpn.*, 1999, **6**, 40–48.
4. Hayashi, H., Hirao, K., Toriyama, M., Kanzaki, S. and Itatani, K., $MgSiN_2$ addition as a means of increasing the thermal conductivity of β-Si_3N_4. *J. Am. Ceram. Soc.*, 2001, **84**, 3060–3062.
5. Lenčéš, Z., Hirao, K., Kanzaki, S., Hoffmann, M. J. and Šajgalík, P., Reaction sintering of fluorine-doped $MgSiN_2$. *J. Eur. Ceram. Soc.*, 2004, **24**, 3367–3375.
6. Gaido, G. K., Dubrovskij, G. P. and Zykov, A. M., Photoluminescence of $MgSiN_2$ activated by europium. *Izv. Akad. Nauk SSSR Neorg. Mater.*, 1974, **10**(3), 564–566.
7. Dubrovskij, G. P., Zykov, A. M. and Tchernovets, B. V., Luminescence properties of rare earth activated $MgSiN_2$. *Izv. Akad. Nauk SSSR Neorg. Mater.*, 1981, **17**(8), 1421–1425.
8. Uheda, K., Takizawa, H., Endo, T., Yamane, H., Shimada, M., Wang, C.-M. *et al.*, Synthesis and luminescent property of Eu^{3+}-doped $LaSi_3N_5$ phosphor. *J. Lumin.*, 2000, **87–89**, 967–969.
9. Ueda, K., Takizawa, H., Endo, T., Yamane, H. and Shimada, M., Synthesis and photoluminescence of the ceramic phosphors using $LaSi_3N_5$ as a host lattice. *Kotai no Hannosei Toronkai Koen Yokoshu*, 1999, **10**, 65–68.
10. Ueda, K., Takizawa, H., Endo, T., Yamane, H., Shimada, M. and Mitomo, M., Synthesis and photoluminescence of lanthanum silicon nitride phosphor doped with cerium. *Nippon Kagakkai Koen Yokoshu*, 2001, **79**, 251.
11. Ellens, A., Fries, T., Fiedler, T. and Huber G., Illumination device with at least one LED as the light source, *European Patent* EP1296376, 26 March 2003.
12. Yoshimura, N., Suehiro, Y., Takahashi, Y., Ota, K., Mitomo, M., Endo, T. *et al.*, Light emitting apparatus and light emitting method. *United States Patent* 20050001225, 6 January 2005.
13. Woike, M. and Jeitschko, W., Preparation and crystal structure of the nitridosilcates $Ln_3Si_6N_{11}$ (Ln = Ce, Pr, Nd, Sm) and $LnSi_3N_5$ (Ln = Ce, Pr, Nd). *Inorg. Chem.*, 1995, **34**(21), 5105–5108.
14. Holcombe, C. E. and Kovach, L., Advanced ceramic materials for hydrogen-fluorine environments. *Am. Ceram. Soc. Bull.*, 1981, **60**(5), 546–548.
15. Inoue, Z., Mitomo, M. and Ii, N., A crystallographic study of a new compound of lanthanum silicon nitride, $LaSi_3N_5$. *J. Mater. Sci.*, 1980, **15**, 2915–2920.
16. Inoue, Z., A new role for nitrogen in silicon nitride and related ceramics. *J. Mater. Sci. Lett.*, 1985, **4**, 656–658.
17. Fanelli, A. J., Solar, J. P., Wu, B. L. and Yamanis, J., Ternary silicon-rare earth nitrides and process for their preparation. *United States Patent* 5292489, 8 March 1994.
18. Hatfield, G. R., Li, B., Hammond, W. B., Reidinger, F. and Yamanis, J., Preparation and characterization of lanthanum silicon nitride. *J. Mater. Sci.*, 1990, **25**(9), 4032–4035.
19. Lenčéš, Z., Hirao, K., Yamauchi, Y. and Kanzaki, S., Reaction synthesis of magnesium silicon nitride powder. *J. Am. Ceram. Soc.*, 2003, **86**(7), 1088–1093.
20. Kresse, G. and Hafner, J., Ab initio molecular dynamics for open-shell transition metals. *Phys. Rev. B*, 1993, **48**, 13115–13118.
21. Kresse, G. and Furthmuller, J., Efficient iterative scheme for ab initio total energy calculations using plane-wave basis set. *Comp. Mater. Sci.*, 1996, **6**, 16–50.
22. Bulanova, M. V., Zheltov, P. N., Meleshevich, K. A., Saltykov, P. A., Effenberg, G. and Tedenac, J.-C., Lanthanum–silicon system. *J. Alloys Comp.*, 2001, **329**, 214–223.
23. Boyer, S. M. and Moulson, A. J., A mechanism for the nitridation of Fe-contaminated silicon. *J. Mater. Sci.*, 1978, **13**, 1637–1646.
24. Lenčéš, Z., Influence of Cr, Fe, Ni and Ti additives on the nitridation kinetics of silicon powder compacts. *Ceram.-Silik.*, 1994, **38**, 61–67.
25. Meschel, S. V. and Kleppa, O. J., Standard enthalpies of formation of some carbides, silicides, germanides and stannides of samarium by high temperature direct synthesis calorimetry. *J. Alloys Comp.*, 1996, **243**, 186–193.
26. Bolgar, A. S., Gorbatschuk, N. P. and Blinder, A. V., Thermodynamic characteristics of lanthanum silicides at high temperatures. *Powder Metall.*, 1994, **3–4**, 48–53 (Russian ed.).
27. Chase Jr., M.W., NIST-JANAF Thermochemical Tables, 4th ed. *J. Phys. Chem. Ref. Data*, Monograph No. 9, 1998.
28. Wada, N., Solin, S. A., Wong, J. and Prochazka, S., Raman and IR absorption spectroscopic studies on α, β and amorphous Si_3N_4. *J. Non-Crystal. Solids*, 1981, **43**, 7–15.
29. Kislyj, P. S., Posunko, L. S. and Malogolovec, V. G., Phase composition of Si_3N_4 powders synthesised by different methods. *Poroshkovaya Metall.*, 1988, **5**, 83–87.
30. Nyquist, R. A. and Kagel, R. O., *Infrared Spectra of Inorganic Compounds*. Academic Press, New York & London, 1971, pp. 114–115.
31. Andrievskij, R. A. and Leontiev, M. A., Phase composition and infrared spectra of Si_3N_4 powders. *Neorg. Mater.*, 1984, **20**(12), 2053–2055.
32. Antsiferov, V. N., Gilyov, V. G. and Karmanov, V. I., IR-spectra and phases structure of sialons. *Vib. Spectrosc.*, 2002, **30**, 169–173.
33. Rebib, F., Tomasella, E., Dubois, M., Cellier, J., Sauvage, T. and Jacquet, M., Structural and optical investigations of SiO_xN_y thin films deposited by RF sputtering. *Surf. Coat. Technol.*, 2005, **200**, 330–333.
34. Benco, L., Hafner, J., Lenčéš, Z. and Šajgalík, P., Electronic structure and bulk properties of β-sialons. *J. Am. Ceram. Soc.*, 2003, **86**, 1162–1167.
35. Benco, L., Hafner, J., Lenčéš, Z. and Šajgalík, P., Density functional study of structures and mechanical properties of Y-doped α-sialons. *J. Eur. Ceram. Soc.*, 2008, **28**, 995–1002.